Original article

Epileptic Disord 2013; 15 (1): 32-43

Clinico-pathological investigations of Rasmussen encephalitis suggest multifocal disease progression and associated focal cortical dysplasia

Dandan Wang [1], Ingmar Blümcke [2], Qiuping Gui [3], Wenjing Zhou [4], Huancong Zuo [4], Jiuluan Lin [4], Yang Luo [4]

[1] Department of Pathology, Xuanwu Hospital, Capital Medical University, Beijing, 100053
[2] Department of Neuropathology, University Hospital Erlangen, Erlangen, Germany
[3] Department of Pathology, PLA General Hospital, Beijing
[4] Department of Neurosurgery, Tsinghua University Yuquan Hospital, Beijing, China

Received August 17, 2012; Accepted December 7, 2012

ABSTRACT – Rasmussen encephalitis is a devastating neurological disorder characterised by seizures, brain inflammation, and progressive hemispheric atrophy. The objective of the current study was to systematically characterise patterns of structural lesions in children with Rasmussen encephalitis, referred for modified anatomical hemispherectomy at the Tsinghua University Epilepsy Center in Beijing. Seven consecutive patients were investigated with a mean age at operation of 4.5 years, who suffered from medically intractable seizures for a mean of 1.6 years. Foci of abnormally increased T2 signal intensity were observed in all patients. With the exception of one child, all patients presented with progressive unilateral cerebral atrophy. FDG-PET imaging revealed extensive regions of hypometabolism within the affected cerebral hemisphere in 3 of 4 patients. Diagnosis of Rasmussen encephalitis was confirmed histologically, demonstrating CD68 positive microglial nodules, as well as CD3 and CD8 positive T lymphocytes invading the cerebral parenchyma. An intriguing observation was the heterogenous distribution of patterns of lesions throughout the affected hemisphere, suggesting multifocal manifestation and distinct sequences of disease progression, from discrete foci of inflammatory infiltrates (stage 1) to extensive cortical destruction (stage 4). Atypical hippocampal sclerosis (HS), with neuronal cell loss affecting most prominently the CA4 region (HS type 3 or end folium sclerosis), was evident in 5 of 7 cases. Four hippocampi also showed chronic inflammation. In addition, we observed associated focal cortical dysplasia (FCD; ILAE type IIId) in 4 of 7 children, supporting the concept of acquired and postmigratory FCD pathomechanisms. Postsurgical seizure freedom was achieved in all children with a mean follow-up period of 2.7 years and continuous antiepileptic medication.

Key words: epilepsy, seizures, neuropathology, inflammation, dysplasia

Correspondence:
Wenjing Zhou
Neurosurgery,
Tsinghua University Yuquan Hospital,
Beijing, China
<closejeo@hotmail.com>

doi:10.1684/epd.2013.0555

Rasmussen encephalitis (RE) is a rare, chronic inflammatory disease of unknown aetiology, affecting mostly children. Focal drug-resistant epilepsy, hemispheric atrophy, progressive intellectual decline, and neurological deficits are common clinical presentations of the disease. A viral cause of RE was suggested by Theodore Rasmussen in 1958 (Rasmussen *et al*., 1958); however, a pathogenic viral agent has so far not been identified. In contrast, auto-antibodies seem to play a pathogenic role (Bauer *et al*., 2012). Elevated levels of autoantibodies directed against subunit 3 of the ionotropic glutamate receptor (GluR3) were first described in 1994 (Rogers *et al*., 1994), but failed to be significant or pathognomic in clinical practice and treatment. These antibodies may instead be characteristic of progressive neuronal cell death during disease progression. These findings do not exclude, however, other humoural pathomechanisms which may play a role in RE. More recently, cytotoxic T cells were demonstrated to directly account for neurodegeneration and astrocytic loss in RE (Bien *et al*., 2002; Bien *et al*., 2005). Immunohistochemical investigations of surgical brain specimens obtained from RE patients consistently revealed CD3+ and CD8+ T lymphocytic infiltrates, providing evidence of granzyme B (GrB)-mediated cytotoxic T lymphocyte attack against neurons. Such T cells containing GrB granules were shown to target neurons (and astrocytes) expressing major histocompatibility complex class I, thereby inducing apoptotic cell death (Bien *et al*., 2002; Bien *et al*., 2005). These findings suggested a potential benefit of anti-inflammatory and immune-suppressive therapy in RE patients in order to attenuate seizures as well as progressive neurological deficits. Indeed, antiepileptic drug treatment failed in most patients and is ineffective against *epilepsia partialis continua* (EPC). On the other hand, immunomodulation, plasmapheresis, and antiviral treatment approaches were reported to be beneficial to only a limited extent. Therefore, epilepsy surgery should be considered in order to effectively control seizures in patients with advanced disease progression. Whereas results of focal resections in RE patients have been disappointing, anatomical or functional hemispherectomies were most successful to control seizures.

Histopathological studies remain, therefore, a valuable resource to further investigate and understand aetiological pathomechanisms and disease progression in RE. Microscopic analysis will usually confirm inflammatory hallmarks of the disease, consisting of widespread perivascular T cell infiltration and microglial nodule formation (Bien *et al*., 2002; Prayson and Frater, 2002; Schwab *et al*., 2009). Neuronal cell death and cortical atrophy are characteristic hallmarks of an advanced disease stage. The extent and pathogenic contribution of other principal brain lesions remains, however, controversial. Previous reports identified a large spectrum of neuropathological alterations, including vascular lesions, tuberous sclerosis or focal cortical dysplasias (FCDs) (Palmer *et al*., 1999; Takei *et al*., 2010). The latter remains an interesting issue with respect to its congenital or acquired origin and pathogenesis, *i.e*. FCD ILAE type I, II, or IIId. The purpose of this study was, therefore, to systematically study the histopathological spectrum of lesions in a series of anatomically well-preserved hemispheres and to correlate these changes with clinical findings and neuroimaging changes in a cohort of 7 consecutive children with RE.

Materials and methods

Patients

Patients with a clinical diagnosis of RE who were referred to the Epilepsy Surgery Center of Tsinghua University Yuquan Hospital, between December 2007 and October 2011, were included in the study. During this time period, the neuropathological diagnosis of RE was made in 7 patients using standard diagnostic criteria, supported by clinical examination, video-EEG monitoring, MRI, and other imaging techniques (Bien *et al*., 2005). Cerebral MRI was performed in our hospital using a 1.5-Tesla machine (Siemens Avanto, Germany). 18F-fluorodeoxyglucose positron emission tomography was performed for 4 patients (Philips Gemini TF, Netherlands). Before surgery, AED treatment lasted for 4 months to 3 years with 2 to 4 antiepileptic drugs tested, including carbamazepine, clonazepam, lamotrigine, levetiracetam, oxcarbazepine, phenobarbital, topiramate, or valproate, but was ineffective to control seizures. All patients received modified anatomical hemispherectomy of the affected hemisphere, as previously described (Adams, 1983; Kral *et al*., 2002; O'Brien *et al*., 2006). Diagnostic brain biopsies were taken for one patient before hemispherectomy. The clinical information of each patient is summarised in *table 1*.

Neuropathological examination

For each patient, the affected hemisphere was anatomically resected and submitted for histopathological review (*figures 1 and 2*). The entire hemisphere was fixed in 10% buffered formalin for one week. The specimen was then anatomically orientated and cut perpendicular to the cortical mantle, frontal to occipital, into 4 mm sections. Samples for histopathological analysis were obtained from each anatomical lobe. Non-epileptic, non-inflammatory brain tissue obtained from autopsy in two patients without neurological disease was used as control and to determine

Table 1. Clinical presentation of patients with Rasmussen encephalitis.

Case No.	Sex	Age at surgery	Onset	Duration	Hemiparesis	Side of affected brain / dominant hemisphere	Mental retardation	Seizure semiology	EEG
1	F	5	3.8	1.2	3	R/L	+	EPC, PS sGS	Abnormal EEG with sharp waves and spike-and-wave complexes in bilateral frontal pole, frontal, central and parietal lobes. All seizures originated in left hemisphere.
2	M	3.5	1.5	2	2	R/L	-	EPC, GS	Abnormal EEG with sharp waves and spike-and-wave complexes in right hemisphere.
3	F	5	4	1	3	L/L	+	EPC, PS	Abnormal EEG with sharp waves and spike-and-wave complexes in left frontal pole , frontal and central lobes, sharp waves in left parietal and temporal lobes.
4	M	11	7	4	4	L/L	+	EPC, PS sGS	Abnormal EEG with sharp waves and spike-and-wave complexes in left central and parietal lobes. All seizures originated in left hemisphere.
5	M	5	1	4	2	R/L	+	EPC, PS	Abnormal EEG in both hemispheres with a slowing-down of waves.
6	M	8	7.2	0.8	0	R/R	+	EPC, PS sGS	Low voltage in right-hemisphere. Abnormal EEG in left hemisphere with a slowing-down of waves, spike waves and sharp waves, especially in left frontal, central and parietal lobe.
7	M	4	3	1	4	R/L	+	EPC, PS	Abnormal EEG with sharp waves and a slowing-down of waves and spike-and-wave complexes in right central, parietal and parietal lobes.

M: male; F: female; R: right; L: left; EPC: *epilepsia partialis continua*; PS: partial seizures; GS: generalised seizures; sGS: secondary generalised seizures.

normal immunohistochemical reactivity patterns. Following routine paraffin embedding (Leica EG1150, Germany), 4-μm thin sections were stained with haematoxylin and eosin (H and E) and Luxol fast blue/HE (LFB/HE). All slides were histopathologically reviewed and abnormal features classified according to Pardo and co-workers (Pardo *et al*., 2004). In addition to the review of H and E-stained material, representative formalin-fixed, paraffin-embedded tissue blocks containing different types of pathological changes

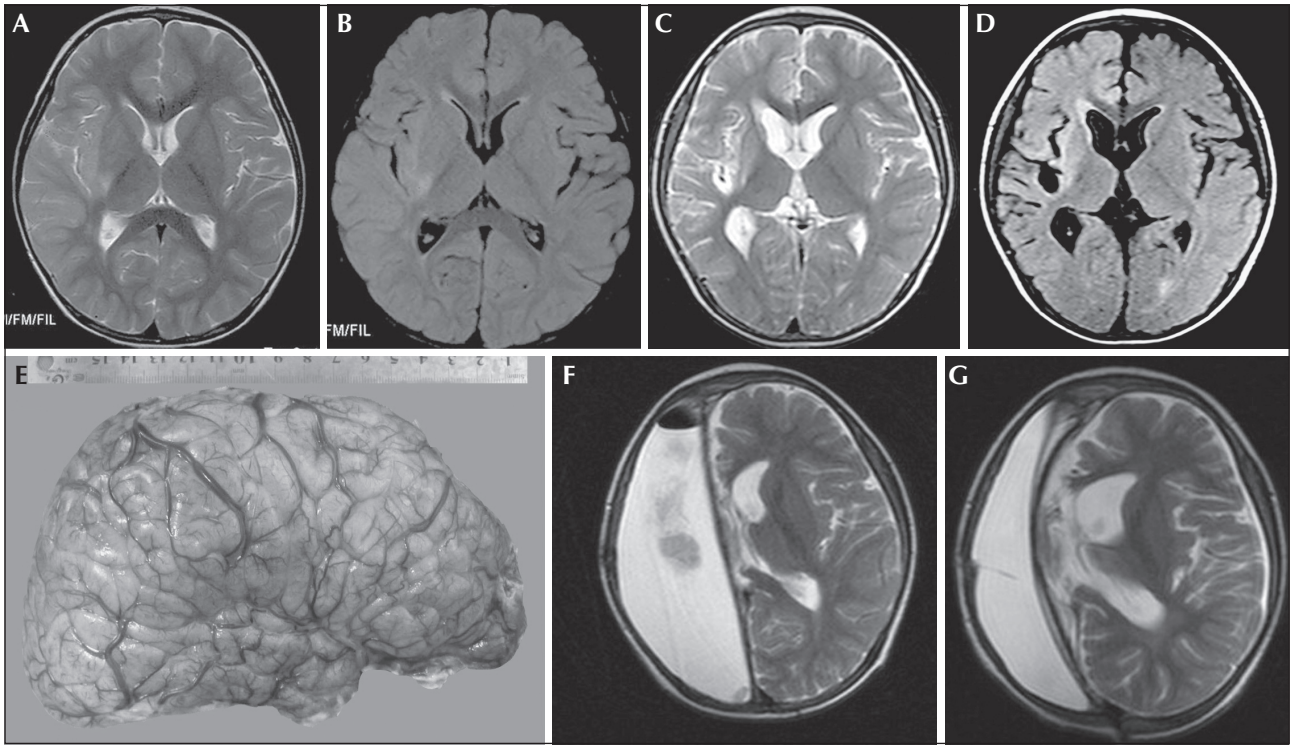

Figure 1. Presentation of Case 2, a 3.5-year-old boy with a two-year history of intractable seizures. Serial axial MRI depicting progressive focal cerebral atrophy 13 months (A and B) and 21 months (C and D) after the first seizure. T2-weighted (A) and Flair (B) revealed signal abnormalities in the posterior right insular lobe. T2 (C) and Flair (D) showed progressive deterioration of signal abnormalities involving the right insular and right frontal lobe. (E) Macroscopic surgical specimen. Serial axial T2-weighted MRI three months (F) and 4 months (G) after modified anatomical hemispherectomy depicting enlargement of the remaining left hemisphere and maintenance of the extradural cavity.

were selected for immunohistochemical procedures. Antibodies against the following molecules were used: CD3, CD4, CD8, CD20, CD79a, CD68, NeuN, Map2, GFAP, SMI-32R, EBV, and NF (see *table 2* for details). The immunohistochemical protocols followed the recommendations given by the manufacturers. All immunohistochemical studies were carried out on paraffin sections which were deparaffinized prior to hydration in graded alcohols, followed by a 5-minute water rinse. A 10-minute wash in 3% hydrogen peroxide at room temperature was also carried out to prevent endogenous peroxidase activity.

Results

Clinical findings

Our study included 5 boys and 2 girls. At the time of surgery, the patients' age ranged from 3.5 to 11 years (with a mean of 4.5 years). All patients had medically intractable seizures at initial examination at hospital, with age at seizure onset ranging from 1.5-7.2 years (mean: 4.4 years). Disease duration varied between 0.8 to 4 years before surgery (mean: 1.6 years). The affected brain region was electroencephalographically localised to the right hemisphere in 5 patients and the left hemisphere in 2 patients. Three features of seizure semiology were noted in our series of patients (see *table 1*): i) seizure polymorphisms in a given patient; ii) all of our patients presented with EPC, which is reported in the literature to occur in 56-92% of patients at some time during the disease course (Bien *et al*., 2005); and iii) medical intractability of seizures, particularly of EPC. In 6 patients, the electroencephalogram (EEG) was abnormal in the affected hemisphere with a slowing-down of background activity and sharp or spike-and-wave discharges (*table 1*). In one additional patient (Case 6), the EEG showed low voltage in the affected hemisphere and abnormal EEG in the contralateral hemisphere, especially in frontal, central, and parietal lobes, including a slowing-down of waves, spike waves, and sharp waves. These findings might relate, however, to the severe atrophy of the affected hemisphere. Bilateral EEG abnormalities were clearly noted in 2 patients and were asymmetrically more pronounced in the affected hemisphere. Four patients with FDG-PET showed an area of abnormal

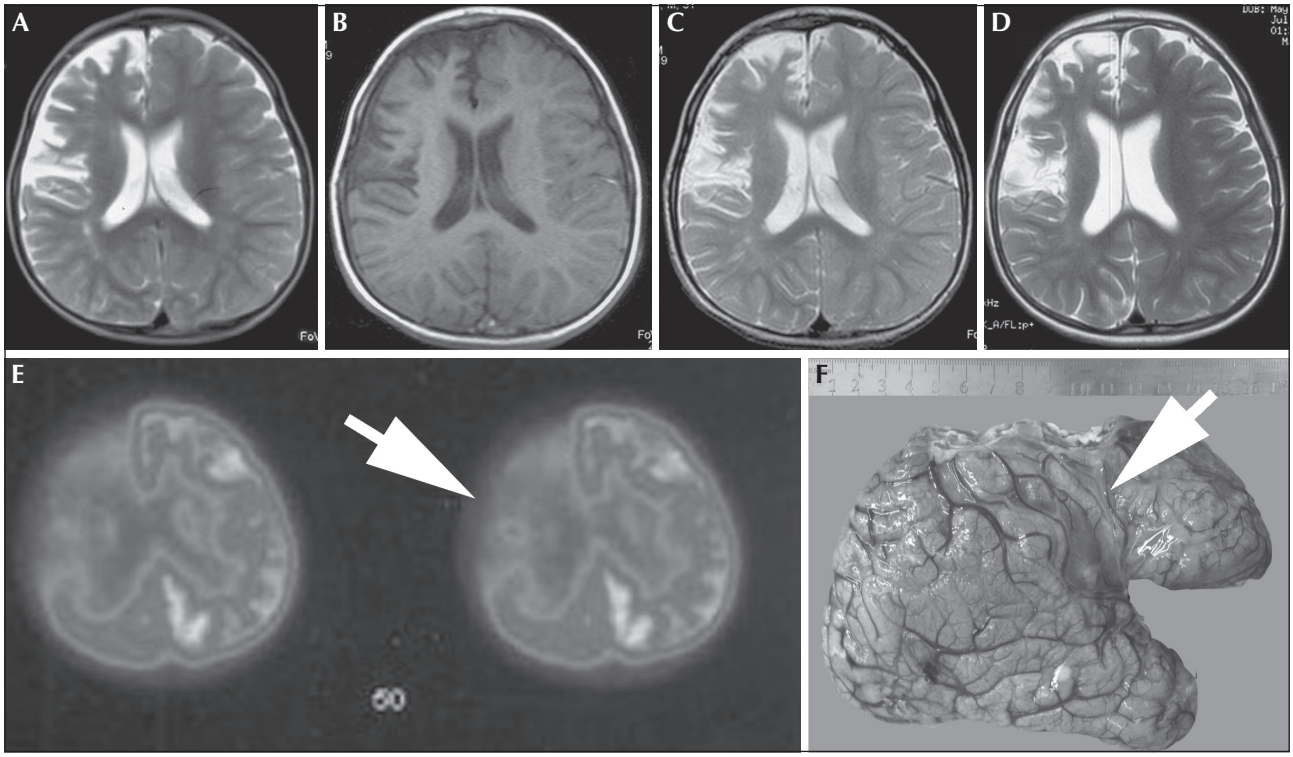

Figure 2. Presentation of Case 7, a 4-year-old boy with a one-year history of intractable seizures. Axial MRI depicts progressive, asymmetrically distributed, sulcal prominence with marked focal atrophy involving the right frontal lobe six months (A), nine months (B and C) and 14 months (D) after the first seizure; T2-weighted images (A, C, D) and T1-weighted images (B). PET images (E) also revealed prominent right hemispheric hypometabolism, which corresponded to marked frontal lobe atrophy visible on the surgical specimen in (F) (indicated by arrows).

Table 2. Antibodies used for immunohistochemical evaluation.

Antibody (clone)	Cellular target	Source	Dilution
CD3(EP449E)	T lymphocytes	DAKO	1:200
CD4(SP35)	$CD4^+$ T lymphocytes	DAKO	1:200
CD8(SP16)	$CD8^+$ T lymphocytes	DAKO	1:100
CD20(L26)	B lymphocytes	DAKO	1:200
CD79a(JCB117)	B lymphocytes	DAKO	1:100
CD68(KP1)	Monocytes, macrophages, microglia	DAKO	1:200
NeuN(A60)	Neuronal nuclei	DAKO	1:200
Map2(AP18)	Neurons	DAKO	1:200
GFAP (ASTR06)	Astrocytes	DAKO	1:100
Neurofilament H non-phosphorylated monoclonal antibody (SMI-32)	Non-phosphorylated neurofilaments	Covance	1:1000
EBV(cs1-4)	Epstein Barr virus	DAKO	1:200
NF(2F11)	Neurofilaments	DAKO	1:200

glucose metabolism corresponding to the anatomical localisation of seizure foci, as determined by clinical assessment and EEG. At the time of first admission to the hospital, no patient presented with hemiparesis. All patients developed hemiparesis later on, coherent with deterioration of neuroimaging findings and disease progression in the affected hemisphere (*table 1*). The degree of hemiparesis was scored according to motor items for the arm or leg using the NIH stroke scale (0=no drift; 1=limb drift; 2=some effort against gravity; 3=no effect against gravity; 4=no movement). Following clinical diagnosis of drug-resistant and progressive RE, surgical treatment was suggested. After interdisciplinary review of clinical findings and discussion with the patients' family, modified anatomical hemispherectomy was performed. Postsurgical follow-up intervals were available at 5 months to 4.3 years (*table 3*). Previous antiepileptic medication was maintained for one year in each patient, followed by dosage decrease or prescription of only one AED. All antiepileptic medication was stopped three years after surgery. No patient reported persisting seizures or auras (Engel class 1a). After surgery, all patients developed contralateral hemiparesis but recovered within one to six months, with better scores than before surgery. Hemianopsia was diagnosed in one patient. All other patients were too young for optic testing. Postsurgical fever was encountered in 4 patients. Postoperative bleeding into the extradural cavity was detected in 5 patients using CT, but did not become clinically symptomatic.

Table 3. Clinical presentation of patients with Rasmussen encephalitis (continued from *table 1* with same case No.)

Case No.	Pre-op MRI	PET	Surgery	Post-op follow-up
1	Atrophy in right frontal and temporal lobes.	Hypermetabolism in right superior frontal gyrus and gyrus frontalis medius, and hypometabolism in the other areas of RCH.	BB, R -MAH	4 years and 6 months: no seizures without medication (Engel class Ia)
2	Atrophy in right frontal and temporal lobes.	-	R -MAH	1 year and 9 months: no seizures with medication (Engel class Ia)
3	Atrophy in left frontal lobe.	Hypometabolism in left frontal, parietal, temporal and occipital lobes, and left thalamus.	L-MAH	4 years and 10 months: no seizures without medication (Engel class Ia)
4	Abnormal high signal in left frontal, temporal, insular, parietal, and occipital lobes.	Hypermetabolism in left frontal, parietal and temporal lobes, left basal ganglia, and thalamus.	L-MAH	4 years and 1 month: no seizures without medication (Engel class Ia)
5	Atrophy in left frontal, temporal, insular, parietal, and occipital lobes.	-	R -MAH	3 years and 9 months: with an episode of seizures at 1.5 years after surgery. Since 9 months seizure-free without medication (Engel class Ib)
6	Extensive atrophy in right hemisphere.	-	R -MAH	5 years and 1 month: with an episode of seizures 2 years after surgery. Seizure-free with dose-reduced medication (Engel class Ib)
7	Atrophy in the right frontal and temple lobe.	Hypometabolism in right frontal, parietal and temporal lobes.	R -MAH	1 year and 3 months: no seizures with medication (Engel class Ia)

BB: brain biopsy; R/L-MAH: right/left-sided modified anatomical hemispherectomy; RCH: right cerebral hemisphere.

Imaging findings

Foci of abnormally increased T2 signal intensity was observed in all patients (*table 3*, *figures 1 and 2*). MRI of all but one patient also showed progressive unihemispheric cortical atrophy. On FDG-PET images, 3 of 4 patients showed extensive regions of hypometabolism within the cerebral hemisphere that showed the greatest atrophy, the distribution of which corresponded to regions of cerebral atrophy on MR images and macroscopic inspection (*figure 2*). One patient had multiple foci of hypermetabolism besides hypometabolism within the cerebral hemisphere. One patient had diffuse unilateral cerebral hypermetabolism distributed within the affected hemisphere. Retrospectively, these signs were not predictive of the presence of associated FCDs. Postsurgical CT was performed 1 to 7 days after surgery, and MRI was performed 12 days to 10 months postoperatively (*figure 1*).

Histological findings

All cases exhibited histopathological hallmarks of RE, *i.e*. severe inflammation and microglial nodules. In addition, 5 cases demonstrated perivascular cuffing by lymphocytes and discrete microglial nodule formations. The vast majority of lymphoid cells observed in our case series were positive for CD3 and CD8, but negative for CD20, CD79a or CD4, which confirmed a T-cytotoxic immunophenotype (*figure 3*). Microglial cells were always positive for CD68 and present in all cases. Immunoreactivity of Epstein Barr viral antigens was negative. Focal cortical atrophy was related to loss of neuronal cells and concomitant astrogliosis, and noted in 4 cases (*figures 3 and 4*). Focal cortical atrophy exactly matched to regions of cerebral atrophy noted on MRI (*figure 2*). Viral inclusion bodies or macrophages were not visible.

Staging of pathological changes in RE was adapted from Pardo *et al*. (2004) and recorded for different

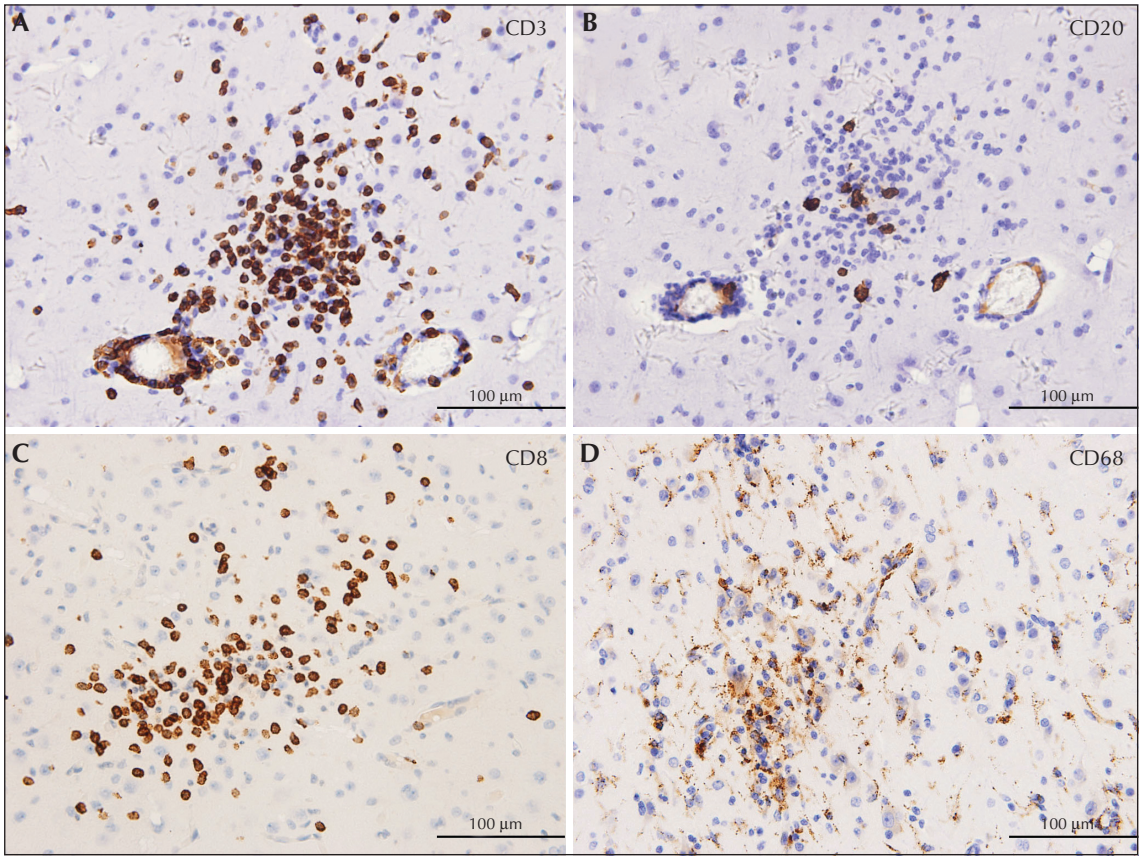

Figure 3. Histopathological hallmarks of Rasmussen encephalitis. Immunohistochemical staining confirmed nodular infiltration of CNS tissue with T lymphocytes (A and C). These cells were mostly characterised as CD3 and CD8 positive cytotoxic killer cells attacking neurons. (B) CD20 staining labelled only few B lymphocytes within inflammatory nodules. (D) CD68 staining revealed the typical formation of microglial nodules in affected cortical areas.
Scale bars: 100 µm.

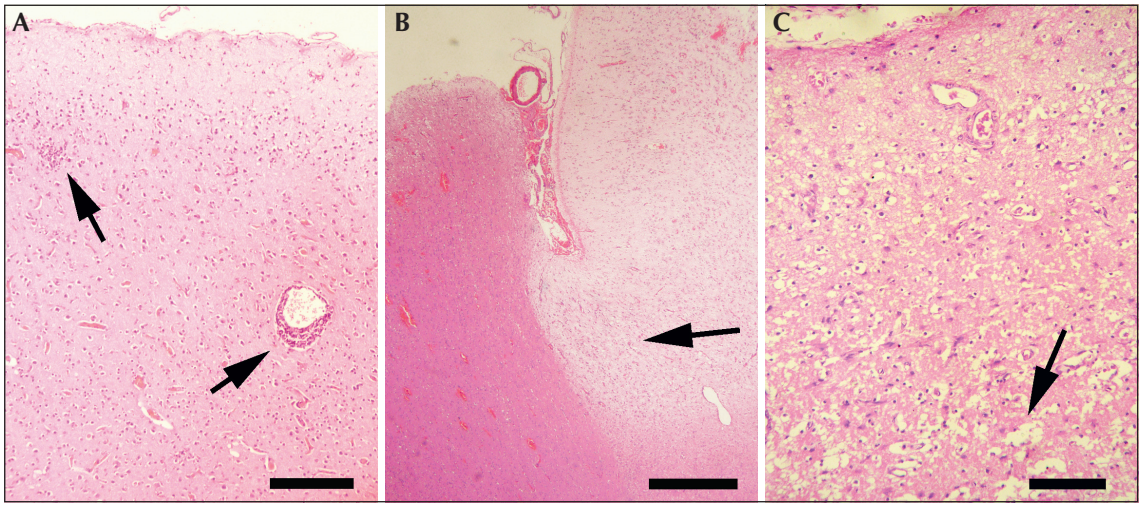

Figure 4. Histopathological stages of neuropathological patterns in RE (H and E staining). (A) Stage 1 was characterised by multifocal distribution of inflammatory changes (arrows); scale bar: 200 μm (applies also to C). (B) In stage 3, severe neuronal loss and astroglial reaction occurred together with brain inflammation (arrow); scale bar: 500 μm. (C) Stage 4 was characterised by prominent cortical atrophy with neuronal loss and astrogliosis. Extensive cortical vacuolation (arrow) was always visible and indicative of this stage.

anatomical regions of the hemisphere (*table 4, figure 4*). Stage 0 represented normal cortex. Stage 1 was defined by discrete foci of inflammatory cells without evidence of cortical or neuronal injury. Stage 2 represented an increase in the magnitude of lymphocytic infiltration as well as the progression of astroglial and microglial reactions from focal areas to panlaminar distribution. Stage 3 was defined by a significant decrease in the neuronal population, either in large focal areas or panlaminar distribution. Stage 4 represented extensive destruction of the cerebral cortex. Our microscopic analysis revealed a heterogeneous distribution of patterns of pathology with different stages, across the various anatomical lobes of the affected hemisphere, suggesting a multifocal and progressive disease manifestation (*table 4*).

FCD type IIId was diagnosed according to the 2011 ILAE classification system of FCD (Blümcke *et al*., 2011), and was present in 4 cases. Case 7 showed abundant microcolumnar organisation of the affected neocortex, as defined by more than 8 immature small-diameter neurons aligned in a vertical direction (*figure 5*). This architectural abnormality was confirmed by immunohistochemistry using antibody against NeuN. Poor demarcation between grey and white matter was also visible. The other 3 cases showed abnormal tangential

Table 4. Clinico-neuropathological findings.

Case No.	Age at surgery	Onset	Duration	Frontal lobe	Temporal lobe	Occipital lobe	Hippocampus	FCD IIId	HS
1	5	3.8	1.2	0	2	1	1	-	HS type 3
2	3.5	1.5	2	4	2	2	2	+	HS type 3
3	5	4	1	2	0	1	0	-	HS type 3
4	11	7	4	3	3	1	0	+	HS type 3
5	5	1	4	4	4	3	0	+	No HS
6	8	7.2	0.8	4	3	4	3	-	HS type 1b
7	4	3	1	4	3	3	2	+	HS type 3

Scores: 0: normal; 1: focal inflammation; 2: inflammation affecting entire cortical width and astrogliosis; 3: severe neuronal cell loss; 4: manifest cortical atrophy. FCD type IIId: focal cortical dysplasia type IIId according to ILAE classification 2011; HS: hippocampal sclerosis (classification according to Blümcke *et al*., 2007). With the exception of Patient 4, early disease onset was associated with FCD type IIId.

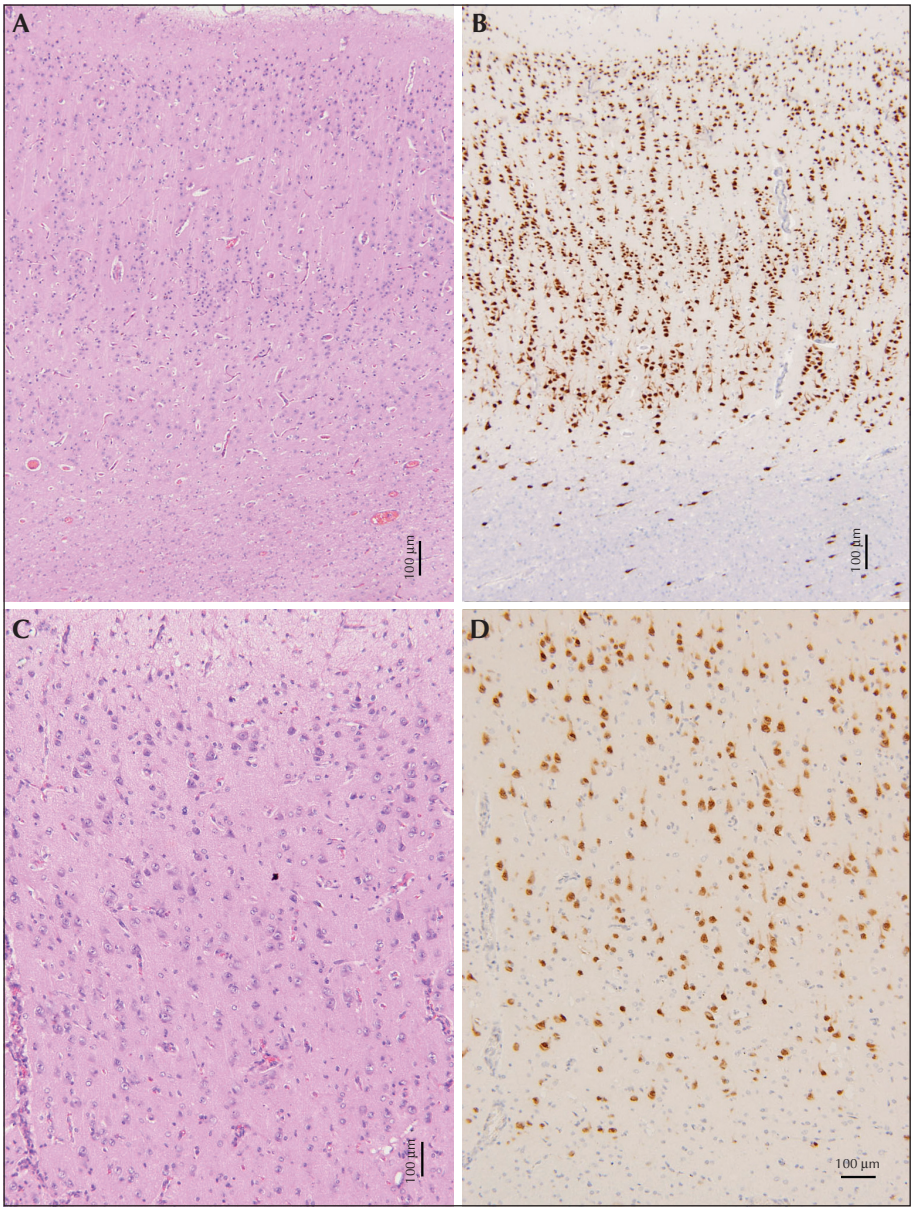

Figure 5. Associated FCD type IIId (ILAE classification 2011). (A and B) Cortex without inflammatory changes (stage 0) revealed FCD with abnormal radial architecture and blurred grey-white matter boundary in Case 7; (A) H and E staining and (B) NeuN staining. (C and D) Cortex with discrete foci of inflammation but no evidence for gross neuronal injury (stage 1) revealed FCD with lack of tangential laminar organisation in Case 2; (C) H and E staining and (D) NeuN staining. Scale bars: 100 µm.

cortical lamination and the entire neocortical architecture was affected. NeuN and Map2 immunostaining confirmed the lack of recognisable layering, with the exception of layer 1 (*figure 5*). Furthermore, these associated FCD type IIId patterns were observed in multiple lobes. Intriguingly, 3 of 4 patients with FCD IIId suffered from very early disease onset (1, 1.5, and 3 years of age, respectively). Neither dysmorphic neurons nor balloon cells were found in this group of children, as confirmed by immunoreactivity for SMI-32R and NF epitopes.

Chronic inflammation and microglial cell proliferation was also observed in 4 specimens from the hippocampal formation. In 6 cases, however, hippocampal sclerosis (HS) was evident (*figure 6*). Microscopically, Cases 1, 2, 3, 4, and 7 showed neuronal loss and reactive gliosis restricted to the CA4 subfield. This pattern is consistent with atypical HS type 3 or endfolium sclerosis, as previously described (Blümcke *et al.*, 2007). Case 6 revealed the classical distribution of segmental neuronal loss and reactive gliosis in CA1, CA3, and CA4 subfields, which was classified as severe

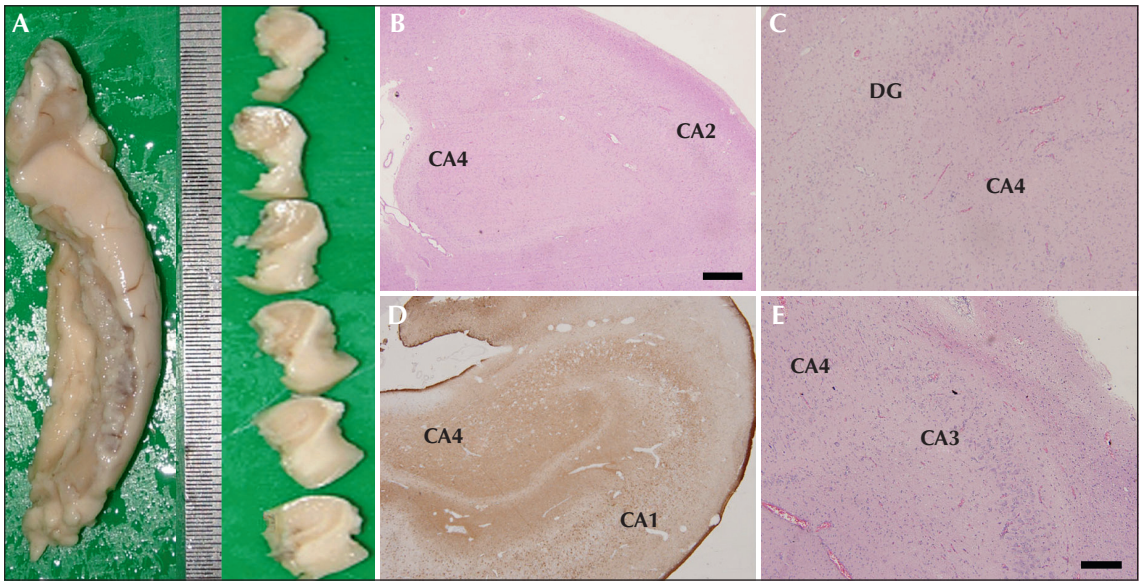

Figure 6. Neuropathological examination of the hippocampal formation in RE patients. (A) Macroscopic examination of surgical hippocampus specimen and serial sections along the anterior-posterior axis revealed no abnormalities (scale in mm). (B and D) Microscopic inspection revealed inflammatory changes, neuronal cell loss, and astrogliosis in CA4, which is compatible with HS type 3 end folium sclerosis. (B, C and E) H and E staining. (D) GFAP staining. Scale bar in (B) is 500 μm (applies also to D) and (E) 200 μm (applies also to C).
Data taken from Case 2.

HS type 1b (Blümcke *et al*., 2007). Only one child (Case 5) presented with an unaffected hippocampus specimen and normal microscopic distribution of pyramidal neurons throughout the hippocampal segments CA1-CA4.

Discussion

RE is a chronic and progressive inflammatory disease, usually affecting one brain hemisphere. Clinico-pathological features of RE included: onset in childhood with a history of intractable epilepsy; the development of slow, progressive, neurological deterioration; radiological evidence of progressive unilateral cerebral atrophy; and pathological features resembling chronic encephalitis. RE is now believed to be an ongoing and progressive immune-mediated process which induces apoptotic neuronal cell death and involves the neuroglial and lymphocytic response, leading to progressive deterioration of a single hemisphere (Pardo *et al*., 2004). Although seen in adulthood, the majority of cases of RE present in childhood with an average age at disease manifestation of 6 years (Oguni *et al*., 1991). In our present series, seizure onset ranged from 1.5-7.2 years, with a mean age of 4.4 years. Establishing the diagnosis of RE is challenging. We applied the criteria proposed by Bien and co-workers (Bien *et al*., 2005), including all of the following clinical parameters: focal seizures with or without EPC and unilateral cortical deficit; unihemispheric slowing-down of EEG with or without epileptiform activity and unilateral seizure onset; MRI showing unihemispheric focal cortical atrophy; and at least one of the following features: grey or white matter T2/FLAIR hyperintense signal, hyperintense signal or atrophy of the ipsilateral caudate head, or additional pathological confirmation of T-cell dominated encephalitis with activated microglial cells and reactive astrogliosis. In this present study, all 7 patients fulfilled all clinical diagnostic criteria and also presented with neuropathological evidence of cytotoxic T lymphocytes infiltrating brain parenchyma.

Medical treatment neither controlled seizures nor significantly affected disease progression in our patients. Since results of focal resections in RE patients were disappointing, we performed modified anatomical hemispherectomy which is considered a highly effective therapy to achieve seizure control in RE (Bien *et al*., 2005). Hemispherectomy is a surgical procedure for total or partial removal of a cerebral hemisphere. Either anatomical or functional hemispherectomies have been proposed (Villemure, 1992; O'Brien *et al*., 2006). Anatomical hemispherectomy involves resection of the whole hemisphere and has been used for the treatment of seizures since 1938. This procedure was abandoned in the 1960s after reports of post-operative mortality caused by hydrocephalus, hemosiderosis, and trivial head traumas (De Almeida *et al*., 2006). Since the era of modified anatomical

hemispherectomy, the incidence of these fatal complications has dramatically decreased and anatomical hemispherectomy should now be perceived as an effective procedure in selective patients (O'Brien *et al*., 2006). We consider very young children to be good candidates for anatomical hemispherectomy. In particular, initial arterial ligation significantly reduces blood loss compared to functional hemispherectomy (Peacock *et al*., 1996). The goal of hemispherectomy is to achieve complete seizure control, promote neurodevelopmental progress in the unaffected contralateral hemisphere, and avoid seizure-related comorbidities. Although all of our patients developed complete hemiparesis after surgery (score=0), they recovered within one to six months (score=2-4), with some patients performing better after surgery. Postoperative seizure freedom rates in RE have been reported between 62.5 and 85% (Vining *et al*., 1997; Kossoff *et al*., 2003; Jonas *et al*., 2004; Pulsifer *et al*., 2004). Our series of 7 young patients achieved complete seizure control without mortality. In addition, cognition and psychomotor development improved according to the physician's assessment as well as parents' observations. In all, the quality of life improved in our group of patients.

Three of 4 patients presented with unilateral cerebral hypometabolism on FDG-PET images. This distribution matched exactly to regions of cerebral atrophy noted on MRI and macroscopic inspection (*figure 2*). One patient (Case 1) showed two foci of hypermetabolism in the superior frontal gyrus and gyrus frontalis medius, and one patient (Case 4) had diffuse unilateral cerebral hypermetabolism. None of these areas with hypermetabolism showed atrophy on MRI. Case 4 showed abnormal high signal in the left frontal, temporal, insular, parietal, and occipital lobes, indicative of seizure activity distributed within the affected hemisphere. Both hypo- and hypermetabolism were located within the affected cerebral hemisphere, allowing the unequivocal identification of the abnormal side in all patients. Histopathological evaluation was most helpful to confirm the clinical diagnosis. In addition, our analysis revealed a heterogeneous distribution of cerebral cortex pathology suggesting multifocal manifestation within the affected hemisphere and distinct sequences of disease progression. In addition, heterogeneity, variability of lesion location, and magnitude of pathological changes were remarkable for each subject as well as between subjects, corroborating previously obtained data (Maeda *et al*., 2003). In this retrospective study, we were not able to correlate pre-operative MRI with histopathology for the same anatomical sections. It was our overall observation that lobar regions found to be atrophic on MRI also revealed significant patterns of pathology, *i.e*. neuronal cell loss (score 3) or cortical atrophy (score 4; *see tables 2 and 3*). However, these findings could not be confirmed for each cortical area in each patient. As an example, atrophy was revealed for Patient 3 in the left cortical lobe (visible by MRI), but showed only inflammation and astrogliosis at the histopathological level. The heterogeneous distribution of patterns of pathology described above may substantially contribute to this discrepancy. Since we did not apply stereological neuronal cell quantification, we may have overlooked less dramatic cell reduction in affected cortical regions, not readily visible by manual microscopic inspection. Our study also demonstrated chronic inflammation and microglial cell proliferation in the hippocampus. The destructive pathogenic process should be considered, therefore, progressive and not restricted to the neocortex.

According to the new ILAE classification system of FCD (Blümcke *et al*., 2011), FCD type IIId associates with lesions acquired during early life, *i.e*. traumatic brain injury, glial scarring after prenatal or perinatal ischaemic injury or bleeding, and inflammatory or infectious diseases. RE is an inflammatory disease and we have identified four patients with FCD type IIId. It is interesting to note that 3 patients with associated FCD type IIId had a very early disease onset at age 1, 1.5, and 3 years, respectively. This finding further supports a role for the concept of acquired and postmigrational pathomechanisms in the aetiology of FCDs (Spreafico, 2010).

It was interesting to note that the atypical pattern of hippocampal neuronal loss and reactive gliosis was restricted to the CA4 subfield in 5 patients (71%). In a previous series of HS patients, atypical patterns were observed in patients with later seizure onset, shorter disease duration, and worse postsurgical outcome (Blümcke *et al*., 2007). Our findings partially contradict these observations, with the exception of a short disease duration in our series of patients. However, there was a prominent clustering of HS type 3 endfolium sclerosis in our RE cohort suggesting a specific aetiological pathomechanism. Neuronal cell death in HS is likely to result from excessive release of excitatory neurotransmitter, which leads to increased depolarisation and calcium overload, thus triggering multiple cell death pathways (Meldrum, 1993). Evidence for a more pronounced level of susceptibility to neuronal damage in CA4 compared to CA1 in RE patients awaits, however, further clarification.

In conclusion, widely distributed pathological findings at different inflammatory stages were observed in the neocortex and hippocampus in children with early RE onset, further supporting the assumption that early treatment by gross removal of the affected hemisphere is beneficial to achieve seizure control of patients with progressive RE. □

Disclosures.
All co-authors declare no conflict of interest. We further confirm that we have read the Journal's position on issues involved in ethical publication and affirm that this report is consistent with those guidelines.
Ingmar Blümcke received financial support from the European EpiGENet consortium (funded by German Research Foundation DFG Bl 421/3-1).

References

Adams CB. Hemispherectomy-a modification. *J Neurol Neurosurg Psychiatry* 1983; 46: 617-9.

Bauer J, Vezzani A, Bien CG. Epileptic encephalitis: the role of the innate and adaptive immune system. *Brain Pathol* 2012; 22: 412-21.

Bien CG, Bauer J, Deckwerth TL, *et al*. Destruction of neurons by cytotoxic T cells: a new pathogenic mechanism in Rasmussen's encephalitis. *Ann Neurol* 2002; 51: 311-8.

Bien CG, Granata T, Antozzi C, *et al*. Pathogenesis, diagnosis and treatment of Rasmussen encephalitis: a European consensus statement. *Brain* 2005; 128: 454-71.

Blümcke I, Pauli E, Clusmann H, *et al*. A new clinico-pathological classification system for mesial temporal sclerosis. *Acta Neuropathol* 2007; 113: 235-44.

Blümcke I, Thom M, Aronica E, *et al*. The clinico-pathological spectrum of focal cortical dysplasias: a consensus classification proposed by an ad hoc Task Force of the ILAE Diagnostic Methods Commission. *Epilepsia* 2011; 52: 158-74.

De Almeida AN, Marino R Jr, Aguiar PH, Jacobsen Teixeira M. Hemispherectomy: a schematic review of the current techniques. *Neurosurg Rev* 2006; 29: 97-102.

Jonas R, Nguyen S, Hu B, *et al*. Cerebral hemispherectomy: hospital course, seizure, developmental, language, and motor outcomes. *Neurology* 2004; 62: 1712-21.

Kossoff EH, Vining EP, Pillas DJ, *et al*. Hemispherectomy for intractable unihemispheric epilepsy etiology *vs* outcome. *Neurology* 2003; 61: 887-90.

Kral T, Clusmann H, Urbach J, *et al*. Preoperative evaluation for epilepsy surgery (Bonn Algorithm). *Zentralbl Neurochir* 2002; 63: 106-10.

Maeda Y, Oguni H, Saitou Y, *et al*. Rasmussen syndrome: multifocal spread of inflammation suggested from MRI and PET findings. *Epilepsia* 2003; 44: 1118-21.

Meldrum BS. Excitotoxicity and selective neuronal loss in epilepsy. *Brain Pathol* 1993; 3: 405-12.

O'Brien DF, Basu S, Williams DH, May PL. Anatomical hemispherectomy for intractable seizures: excellent seizure control, low morbidity and no superficial cerebral haemosiderosis. *Childs Nerv Syst* 2006; 22: 489-98; discussion: 99.

Oguni H, Andermann F, Rasmussen TB. The natural history of the syndrome of chronic encephalitis and epilepsy: a study of the MNI series of fortyeight cases. In: Andermann F. *Chronic encephalitis and epilepsy*. Boston: Butterworth-Heinemann, 1991: 7-35.

Palmer CA, Geyer JD, Keating JM, *et al*. Rasmussen's encephalitis with concomitant cortical dysplasia: the role of GluR3. *Epilepsia* 1999; 40: 242-7.

Pardo CA, Vining EP, Guo L, Skolasky RL, Carson BS, Freeman JM. The pathology of Rasmussen syndrome: stages of cortical involvement and neuropathological studies in 45 hemispherectomies. *Epilepsia* 2004; 45: 516-26.

Peacock WJ, Wehby-Grant MC, Shields WD, *et al*. Hemispherectomy for intractable seizures in children: a report of 58 cases. *Childs Nerv Syst* 1996; 12: 376-84.

Prayson RA, Frater JL. Rasmussen encephalitis: a clinicopathologic and immunohistochemical study of seven patients. *Am J Clin Pathol* 2002; 117: 776-82.

Pulsifer MB, Brandt J, Salorio CF, Vining EP, Carson BS, Freeman JM. The cognitive outcome of hemispherectomy in 71 children. *Epilepsia* 2004; 45: 243-54.

Rasmussen T, Olszewski J, Lloydsmith D. Focal seizures due to chronic localized encephalitis. *Neurology* 1958; 8: 435-45.

Rogers SW, Andrews PI, Gahring LC, *et al*. Autoantibodies to glutamate receptor GluR3 in Rasmussen's encephalitis. *Science* 1994; 265: 648-51.

Schwab N, Bien CG, Waschbisch A, *et al*. CD8+ T-cell clones dominate brain infiltrates in Rasmussen encephalitis and persist in the periphery. *Brain* 2009; 132: 1236-46.

Spreafico R. Are some focal cortical dysplasias post-migratory cortical malformations? *Epileptic Disord* 2010; 12: 169-71. doi: 10.1684/epd.2010.0331

Takei H, Wilfong A, Malphrus A, *et al*. Dual pathology in Rasmussen's encephalitis: a study of seven cases and review of the literature. *Neuropathology* 2010; 30: 381-91.

Villemure JG. Anatomical to functional hemispherectomy from Krynauw to Rasmussen. *Epilepsy Res Suppl* 1992; 5: 209-15.

Vining EP, Freeman JM, Pillas DJ, *et al*. Why would you remove half a brain? The outcome of 58 children after hemispherectomy-the Johns Hopkins experience: 1968 to 1996. *Pediatrics* 1997; 100: 163-71.